Field Induced Transition and Behavior of the Phase Front in $Pb(Zn_{1/3}Nb_{2/3})O_3$-8%$PbTiO_3$

Makoto IWATA[a] and Yoshihiro ISHIBASHI[b]

[a]*Department of Engineering Physics, Electronics and Mechanics, Graduate School of Engineering, Nagoya Institute of Technology, Nagoya 466-8555, Japan;*

[b]*Department of Physics, Kyushu University, Hakozaki, Higashi-ku, Fukuoka, 812-8581, Japan*

(Received:)

Field induced phase transition in $Pb(Zn_{1/3}Nb_{2/3})O_3$-8%$PbTiO_3$ was investigated by measuring temperature dependence of the dielectric constant under the DC biasing field. It was clarified that the critical end point (CEP) exists at 170 ± 2^oC and 1.5 ± 0.2 kV/cm. The boundary between the ferroelectric and the paraelectric phases near CEP was discussed on the basis of the Landau-type free energy. It is confirmed that the wall width is in proportion to $(E_{ce} - E)^{-1/2}$, and diverges at CEP ($E = E_{ce}$), where E is the electric field and E_{ce} is E at CEP.

KEYWORDS： PZN, relaxor, ferroelectric, morphotropic phase boundary, phase diagram, critical end point

Corresponding author. Email: miwata@nitech.ac.jp

1. Introduction

It is well-known that mixed crystals of Pb based relaxors and ferroelectric $PbTiO_3$ show giant dielectric and piezoelectric responses near the morphotropic phase boundary (MPB). Among them, $Pb(Zn_{1/3}Nb_{2/3})O_3$-$x$$PbTiO_3$ (PZN-xPT) shows MPB at x = 8-9% at room temperature [1]. With respect the giant response near MPB, in the early stages, Carl and Hardtl discussed the enhancement of the dielectric constant perpendicular to the spontaneous polarization in $Pb(Zr,Ti)O_3$ (PZT) based on the Landau-type free energy [2]. It was claimed that such giant responses essentially come from the transversal instability near MPB on the basis of the Landau-type free energy, where the dielectric constant perpendicular to the spontaneous polarization becomes extremely large because anisotropy of the free energy in the parameter space becomes small [2-4]. It was also reported on the basis of the first principles studies that a similar mechanism for such giant response exists in $BaTiO_3$ [5]. On the experimental side, we confirmed that the dielectric constant perpendicular to the spontaneous polarization in PZN-xPT significantly increases with approaching MPB [6]. Furthermore, it was reported that physical properties near MPB in PZN-xPT are sensitive to external fields such as stresses and electric fields, reflecting that the giant dielectric and piezoelectric responses are due to the transversal instability [7,8].

On the other hand, it was found that a new sharp phase transition at 114^{o}C below the paraelectric-ferroelectric phase transition point in PZN appears only on zero-field heating (ZFH) after field cooling (FC) process [9,10]. We reported a new phase diagram in poled samples of PZN-xPT, and found that the new sharp transition in the poled PZN and the transition at MPB are the same kind, showing that this new transition corresponds to that between the tetragonal and rhombohedral phases [11-13]. We claimed that the nature of the phase transition smeared by complex domain structures such as a polar nanoregion (PNR) can be clarified by decreasing heterogeneity owing to the electric field on the FC process.

Recently, Kutnjak *et al*. experimentally discovered the critical end point (CEP) on the three dimensional concentration-temperature-field phase diagram in $Pb(Mg_{1/3}Nb_{2/3})O_3$-$x$$PbTiO_3$ (PMN-

*x*PT), and claimed that the giant electromechanical response in PMN-*x*PT is the manifestation of CEP in addition to MPB [14]. These phase transitions were discussed on the basis of the Landau-type free energy, and it was shown that the fourth order anisotropy of the polarization in the free energy plays an important role in the determination of the aspect in this phase diagram [15,16]. Many experimental results with respect to CEP in PMN-*x*PT were reported to clarify its detail [17-21]. We have confirmed the existence of CEP in PZN-8%PT to clarify the nature of the phase transition under the electric field [22-25]. In this paper, we summarize our experimental data with respect to temperature-field phase diagram and discuss physical properties of the phase front (phase boundary between the paraelectric and ferroelectric phases) on the basis of the Landau-type free energy.

2. Experimental procedure and results

Single crystals of PZN-8%PT used for our experiments were acquired from Microfine Technologies in Singapore, where the size of the platelike sample is $3\times3\times0.4$ mm^3 perpendicular to the [001] direction in the cubic coordinate. For the measurement of the dielectric constant, the (001)-crystal plates in the cubic coordinate with Au electrodes deposited on their faces were prepared. Measurements of the dielectric constant with and without the dc biasing field were carried out using an LCR hi-tester (Hioki 3532-50), where the temperature changes at a rate of 2 K/min.

Figure 1 shows temperature dependences of the dielectric constants along the [001] direction in PZN-8%PT on cooling, where the DC biasing fields, E, are 0, 1.0, 1.5, 2.5 kV/cm. It is found that two anomalies showing the phase transitions appear in each figure. These are attributed to the cubic-tetragonal and tetragonal-rhombohedtral phase transitions, respectively. It is seen that the broad peak showing the cubic-tetragonal transition at $E = 0$ changes to the sharp phase transition with approaching about $E = 1.5$ kV/cm, and above 1.5 kV/cm, a broad peak appears again. This indicates that CEP exists around $E = 1.5$ kV/cm.

Figure 2 shows temperature-field phase diagram under the electric field along the [001]

direction in PZN-8%PT. It is seen that due to the electric field along the [001] direction, the region of the tetragonal phase increases with increasing the field, and CEP on the phase diagram is found at 170 ± 2^{o}C and 1.5 ± 0.2 kV/cm. Note that the critical field to be about 1.5 kV/cm is very small compared with that in ordinary perovskite ferroelectrics such as $BaTiO_3$. The slope of the phase boundary between the cubic and tetragonal phases was estimated to be about $dE/dT = 0.2$ kV/cmK.

3. Discussion

In the present study, we clarified the temperature-field phase diagram along the [001] direction, and confirmed the existence of CEP in PZN-8%PT. The phase diagram was qualitatively reproduced on the basis of the Landau-type free energy [21].

In this section, we consider the boundary between the ferroelectric and the paraelectric phases near CEP, which we call the phase front. We only consider the static structure of the phase front by assuming the static coexistence just at the first order transition point. The Landau-type free energy density under the applied field is written as

$$f = \frac{\alpha}{2} p^2 + \frac{\beta}{4} p^4 + \frac{\gamma}{6} p^6 - pE + \frac{\kappa}{2}\left(\frac{dp}{dx}\right)^2, \qquad (1)$$

where p and E are the z components of the polarization $\boldsymbol{p} = (0, 0, p)$ and electric field $\boldsymbol{E} = (0, 0, E)$, respectively, and α represents the temperature, β (< 0) and γ (> 0) are constants, κ (> 0) expresses the increase in the free energy due to the inhomogeneity of polarization. The total free energy is given by

$$F = \int_{-\infty}^{\infty} f(x)dx. \qquad (2)$$

In the homogeneous case ($dp/dx = 0$), the first order phase transition under no applied field occurs at $\alpha_c = 3\beta^2/16\gamma$, and CEP is located at $\alpha_{ce} = 9\beta^2/20\gamma$ and $E_{ce} = (6\beta^2/25\gamma)\sqrt{-3\beta/10\gamma}$ [14].

The modulation structure of the phase front can be obtained using the Euler-Lagrange equation, $\delta F/\delta p = 0$, i.e.,

$$\alpha p + \beta p^3 + \gamma p^5 - \kappa \frac{\mathrm{d}^2 p}{\mathrm{d}x^2} = E \qquad (3)$$

under the boundary conditions

$$p(x) = p_1 \quad \text{at } x = -\infty,$$

$$p(x) = p_2 \quad \text{at } x = \infty, \qquad (4)$$

where p_1 and p_2 ($p_1 < p_2$) are the stable polarization values at the first order transition point (see Fig. 3). Hereafter, we call the phase characterized by p_1 the paraelectric phase because $p_1 = 0$ under no applied field. Note that the free energy density in the paraelectric phase $f(p_1)$ coincides with that in the ferroelectric phase $f(p_2)$ just at the first order transition point.

Figure 4 shows the numerical results of the spatial modulation structure $p(x)$ near the phase boundary between the ferroelectric phase and paraelectric phase at the transition point. The parameter values are $\beta = -1$, $\gamma = 1$, $\kappa = 1$, and in (a) $\alpha = 0.1875$ and $E = 0$, in (b) $\alpha = 0.3$ and $E = 0.05278$, and in (c) $\alpha = 0.43$ and $E = 0.12038$. The dotted line shows the fit of the function,

$$p(x) = p_0 + p_A \tanh Kx, \qquad (5)$$

where

$$p_0 = \frac{p_2 + p_1}{2} \quad \text{and} \quad p_A = \frac{p_2 - p_1}{2}, \qquad (6)$$

and K is the inverse domain wall width. It is seen that eq. (5) is a good approximation for the spatial modulation structure near CEP, and the wall width ($1/K$) increases with approaching CEP ($E = E_{ce}$) analytically.

Next, let us consider the field, $E_{ce} - E$, dependence of the wall width ($1/K$) near CEP. The inverse wall width K can be estimated as

$$K = \frac{2}{p_2 - p_1}\left(\frac{\mathrm{d}p}{\mathrm{d}x}\right)_{\max}, \qquad (7)$$

where $(\mathrm{d}p/\mathrm{d}x)_{\max}$ is the maximum value of the $\mathrm{d}p/\mathrm{d}x$, and p_1 and p_2 are the stable values of the polarizations at the first order transition point (see Fig. 3). Integrating the Euler-Lagrange equation in eq. (3) under the boundary conditions in eq. (4), we obtain

$$\frac{\alpha}{2}p^2+\frac{\beta}{4}p^4+\frac{\gamma}{6}p^6-pE-f_1=\frac{\kappa}{2}\left(\frac{\mathrm{d}p}{\mathrm{d}x}\right)^2, \tag{8}$$

where $f_1 = f(p_1) = f(p_2)$. The square of $(\mathrm{d}p/\mathrm{d}x)_{\max}$ is written as

$$\left(\frac{\mathrm{d}p}{\mathrm{d}x}\right)^2_{\max}=\frac{2}{\kappa}\left[\frac{\alpha}{2}p_{\mathrm{m}}^2+\frac{\beta}{4}p_{\mathrm{m}}^4+\frac{\gamma}{6}p_{\mathrm{m}}^6-p_{\mathrm{m}}E-\left(\frac{\alpha}{2}p_1^2+\frac{\beta}{4}p_1^4+\frac{\gamma}{6}p_1^6-p_1E\right)\right], \tag{9}$$

where p_{m} is the polarization corresponding to the maximum of the free energy (see Fig.3). Using the relations in eqs. (3), (7)-(9), K^2 can be expanded by the power series of $E_{\mathrm{ce}} - E$ around CEP. If we only take the first order term of the field $E_{\mathrm{ce}} - E$ near CEP, the square of K is approximately written as

$$K^2\approx\frac{1}{2\kappa}\left(\frac{\mathrm{d}\alpha}{\mathrm{d}E}\right)_{E=E\mathrm{ce}}\left(E_{\mathrm{ce}}-E\right), \tag{10}$$

where the derivative $\mathrm{d}\alpha/\mathrm{d}E$ is taken along the line of the first order transition. This indicates that the domain wall width diverges with approaching CEP in proportion to $(E_{\mathrm{ce}} - E)^{-1/2}$. The derivation of eq. (10) will be published elsewhere. Figure 5 shows a numerical result of the electric field, E, dependence of the K^2 obtained from results of the fitting in eq. (5). It is also confirmed numerically that the wall width $(1/K)$ is in proportion to $(E_{\mathrm{ce}} - E)^{-1/2}$, and diverges at CEP ($E = E_{\mathrm{ce}}$).

In general, in relaxors, the ferroelectric and paraelectric phases coexist, and the ferroelectric region in the paraelectric matrix is called PNR. From our theory, we found that the width of the phase front between ferroelectric and paraelectric phases increases in proportion to $(E_{\mathrm{ce}} - E)^{-1/2}$. It can be guessed that the PNR and matrix cannot be distinguished near CEP, because the width of the phase front in the PNR becomes very thick near CEP. We point out that the contribution from the phase front between the feroelectric and the patraelectric phases near CEP may play an important role in the large dielectric responses.

Acknowledgement

This work was supported in part by Grants-in-Aid for Scientific Research (B) (No.

22340081) from the Japan Society for the Promotion of Science for MI.

References

[1] J. Kuwata, K. Uchino, and S. Nomura: Jpn. J. Appl. Phys. **21** (1982), pp. 1298-1302.

[2] K.Carl and K. H. Hardtl: Phys. Stat. Sol. (a) **8** (1971) pp. 87-98.

[3] Y. Ishibashi and M. Iwata: Jpn. J. Appl. Phys. **37** (1998), pp. L985-L987.

[4] M. Iwata and Y. Ishibashi: Ferroelectric Thin Films, eds. M. Okuyama and Y. Ishibashi (Springer, 2005) Part III, p. 127.

[5] H. Fu and R. E. Cohen: Nature **403** (2000), pp. 281-283.

[6] M. Iwata, K. Sakakibara, K. Katsuraya, R. Aoyagi, M. Maeda, I. Suzuki, and Y. Ishibashi: Jpn. J. Appl. Phys. **45** (2006), pp. 7543-7547.

[7] M. Iwata, Y. Hasegawa, M. Maeda, N. Yasuda, and Y. Ishibashi: Jpn. J. Appl. Phys. **44** (2005), pp. 7165-7168.

[8] M. Iwata, T. Araki, M. Maeda, I. Suzuki, H. Ohwa, N. Yasuda, H. Orihara, and Y. Ishibashi: Jpn. J. Appl. Phys. **41** (2002), pp. 7003-7006.

[9] Y.-H. Bing, A. A. Bokov, Z.-G. Ye, B. Niheda, and G. Shirane: J. Phys.: Condens. Matter **17** (2005), pp. 2493-2507.

[10] S. Wada, T. Tsurumi, S.-E. Park, L. E. Cross and T. R. Shrout: Trans. Mater. Res. Soc. Jpn. **25** (2000), pp. 281-284.

[11] M. Iwata, K. Katsuraya, R. Aoyagi, M. Maeda, I. Suzuki, and Y Ishibashi: Jpn. J. Appl. Phys. **46** (2007), pp. 2991-2994.

[12] M. Iwata, K. Sakakibara, R. Aoyagi, M. Maeda, and Y. Ishibashi: J. Ceramic Soc. Jpn. **117** (2009), pp. 954-957.

[13] M. Iwata, K. Kuroda, Y. Hasegawa, R. Aoyagi, M. Maeda, Y. Ishibashi: Jpn. J. Appl. Phys. **48** (2009), 09KF07 (pp. 1-5).

[14] Z. Kutnjak, J. Petzelt, and R. Blinc: Nature **441** (2006), pp. 956-959.

[15] M. Iwata, Z. Kutnjak, Y. Ishibashi and R. Blinc: J. Phys. Soc. Jpn. **77** (2008), 034703 (pp. 1-6).

[16] M. Iwata, Z. Kutnjak, Y. Ishibashi and R. Blinc: J. Phys. Soc. Jpn. **77** (2008), 065003 (pp. 1-2).

[17] Z. Kutnjak, R. Blinc, Y. Ishibashi: Phys. Rev. B **76** (2007), 104102 (pp. 1-8).

[18] S. I. Raevskaya, A. S. Emelyanov, F. I. Savenko, M. S. Panchelyuga, I. P. Raevski, S. A. Prosandeev, E. V. Colla, H. Chen, S. G. Lu, R. Blinc, Z. Kutnjak, P. Gemeiner, B. Dkhil, and L. S. Kamzina: Phys. Rev. B **76** (2007), 060101(R) (pp. 1-4).

[19] B. E. Vugmeister and H. Rabitz: Phys. Rev. B **65** (2001), 024111 (pp. 1-4).

[20] B. Dkhil and J. M. Kiat: J. Appl. Phys. **90** (2001), pp. 4676-4681.

[21] X. Zhao, W. Qu, X. Tan, A. A. Bokov, and Z.-G. Ye: Phys. Rev. B **75** (2007), 104106 (pp. 1-12).

[22] M. Iwata, N. Iijima, and Y. Ishibashi: to be published in Jpn. J. Appl. Phys. **49** (2010).

[23] M. Iwata, S. Kato, and Y. Ishibashi: to be published in Ferroelectrics.

[24] M. Iwata, S. Kato, and Y. Ishibashi: submitted to Current Applied Physics.

[25] M. Iwata, S. Kato, and Y. Ishibashi: submitted to J. Korean. Phys. Soc.

Figure 1 Temperature dependence of the dielectric constant in the (001)-plate of PZN-8%PT measured on cooling. The biasing DC fields, E, are 0, 1.0, 1.5, and 2.5 kV/cm.

Figure 2 Temperature-field phase diagram in PZN-8%PT. The electric field is along the [001] direction in the cubic coordinate. Open and solid circles indicate the transition point from the dielectric constant measured on heating and cooling, respectively. Open squares indicate the transition point from electrostriction loops [24]. Solid square indicates CEP.

Figure 3 An example of the free energy function at the first order transition pint. The parameter values are $\beta = -1$, $\gamma = 1$, $\alpha = 0.35$, and $E = 0.0782$.

Figure 4 Numerical results of the spatial modulation structure near the phase boundary between the ferroelectric phase and paraelectric phase at the transition point. The dotted line shows the fit of the function, $p_0 + p_1 \tanh Kx$. The parameter values are $\beta = -1$, $\gamma = 1$, $\kappa = 1$, and in (a) $\alpha = 0.1875$ and $E = 0$, in (b) $\alpha = 0.3$ and $E = 0.05278$, and in (c) $\alpha = 0.43$ and $E = 0.12038$.

Figure 5 The electric field dependence of K^2. The electric field at CEP is $E_{ce} = 0.1314$.

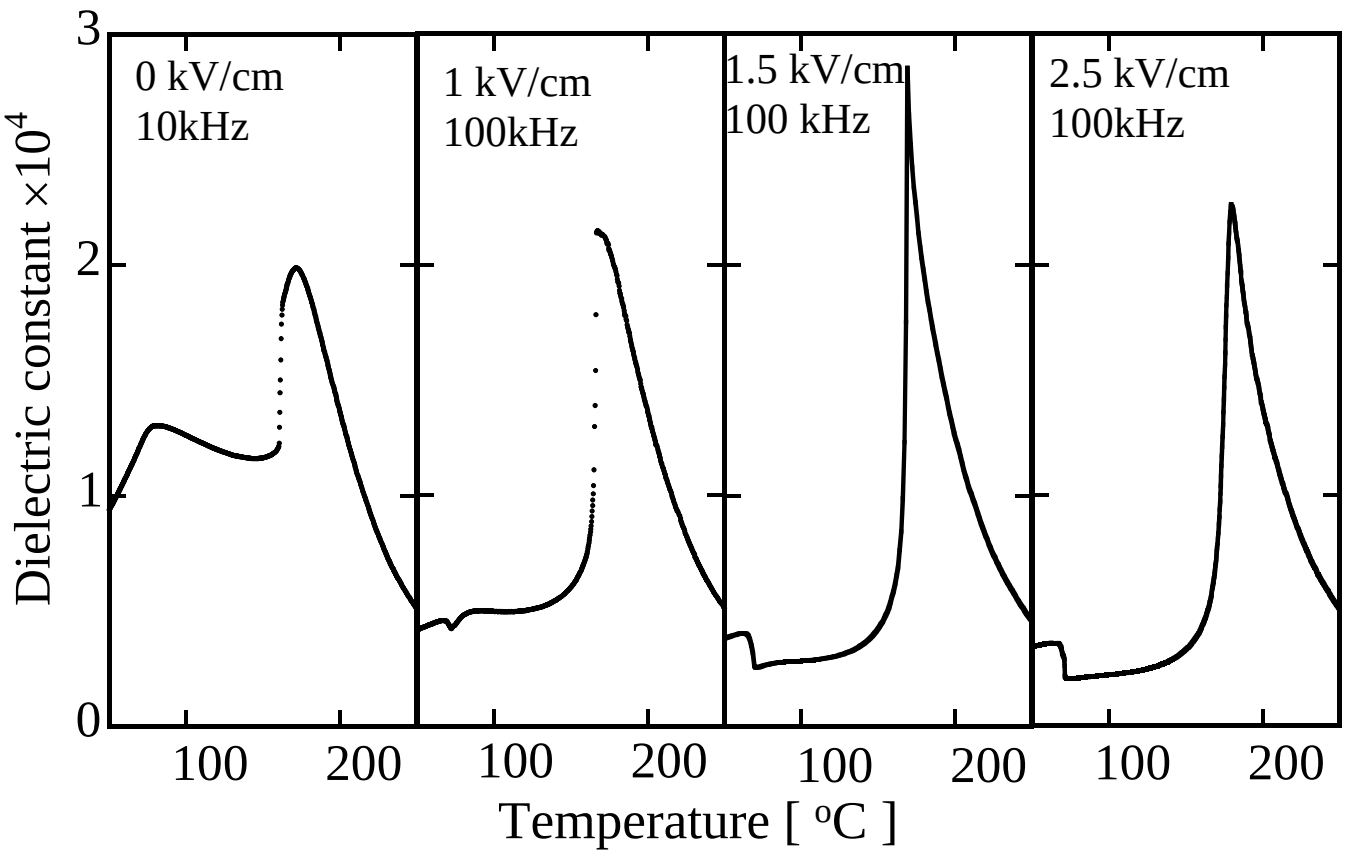

Fig. 1 M. Iwata and Y. Ishibashi

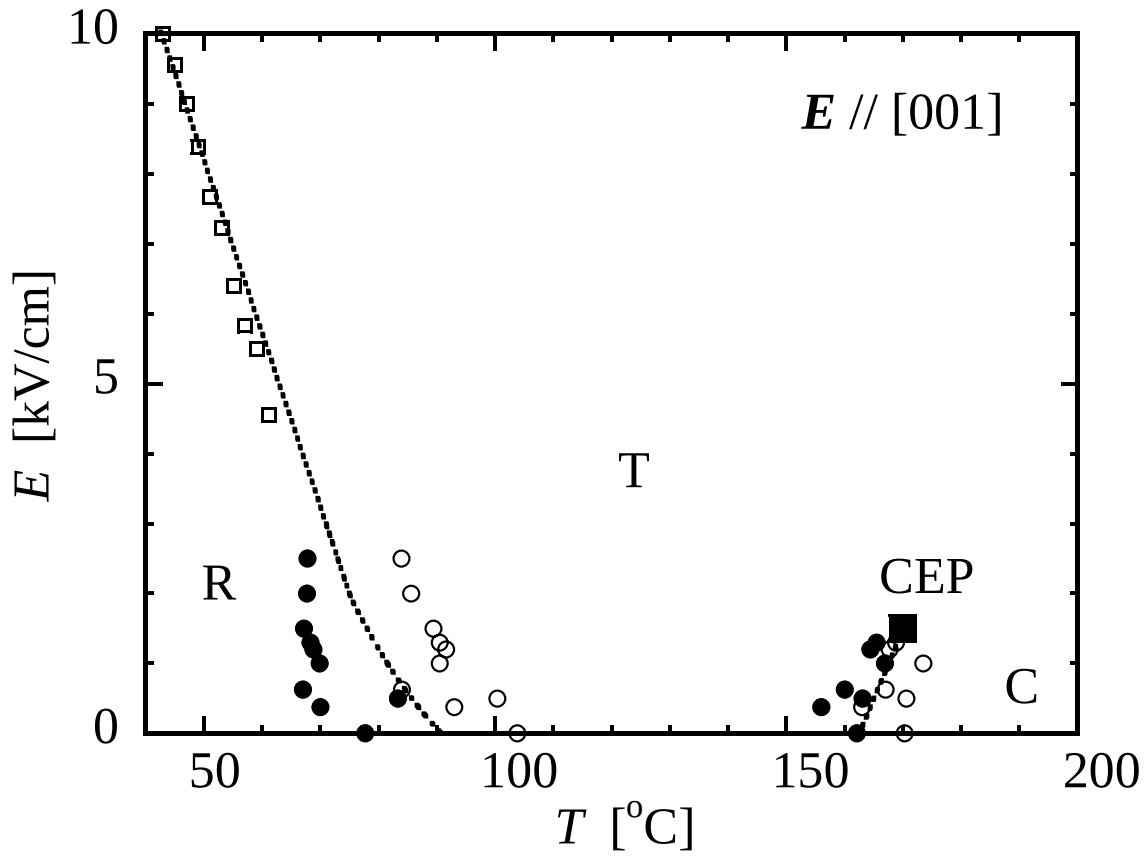

Fig. 2 M. Iwata and Y. Ishibashi

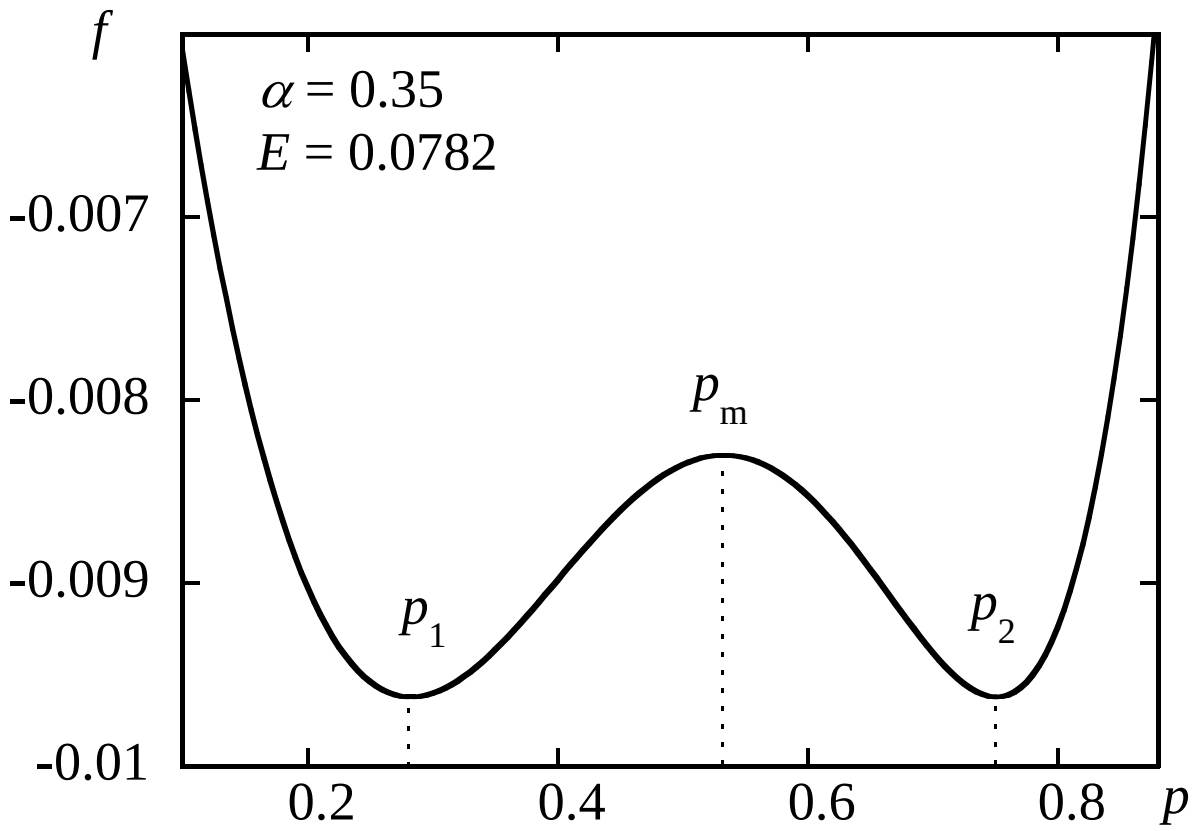

Fig. 3 M. Iwata and Y. Ishibashi

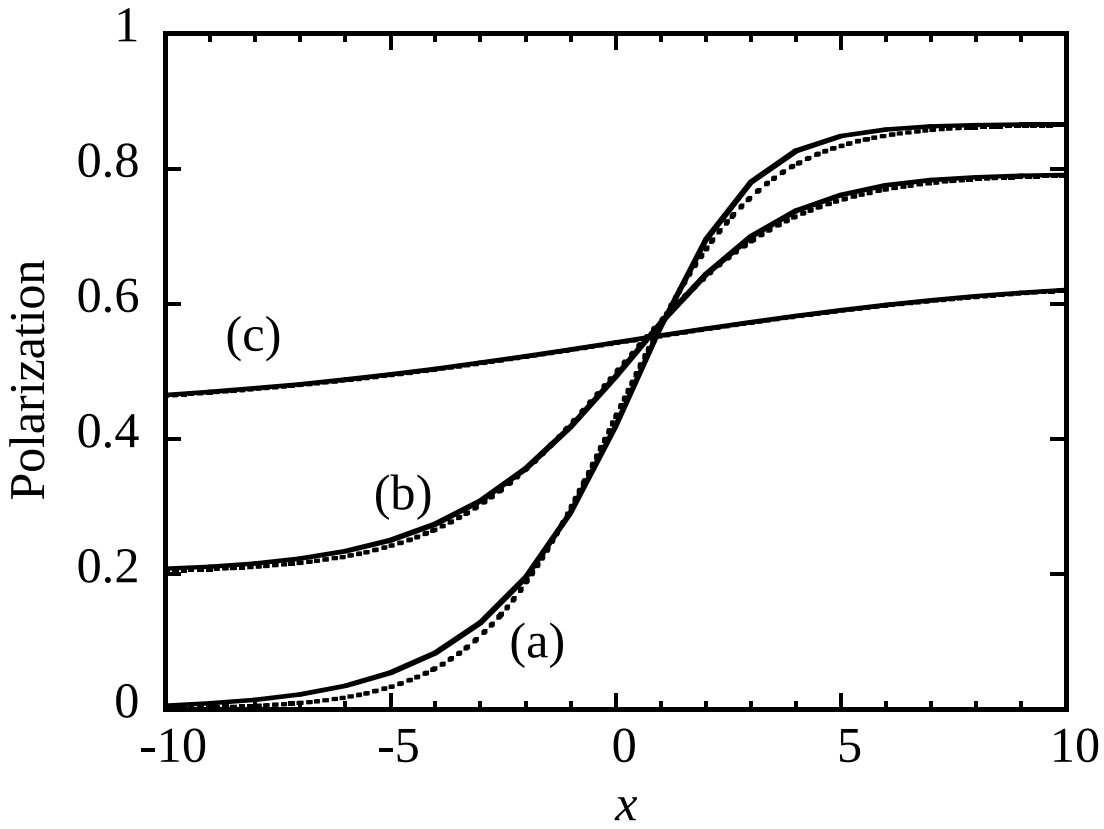

Fig. 4 M. Iwata and Y. Ishibashi

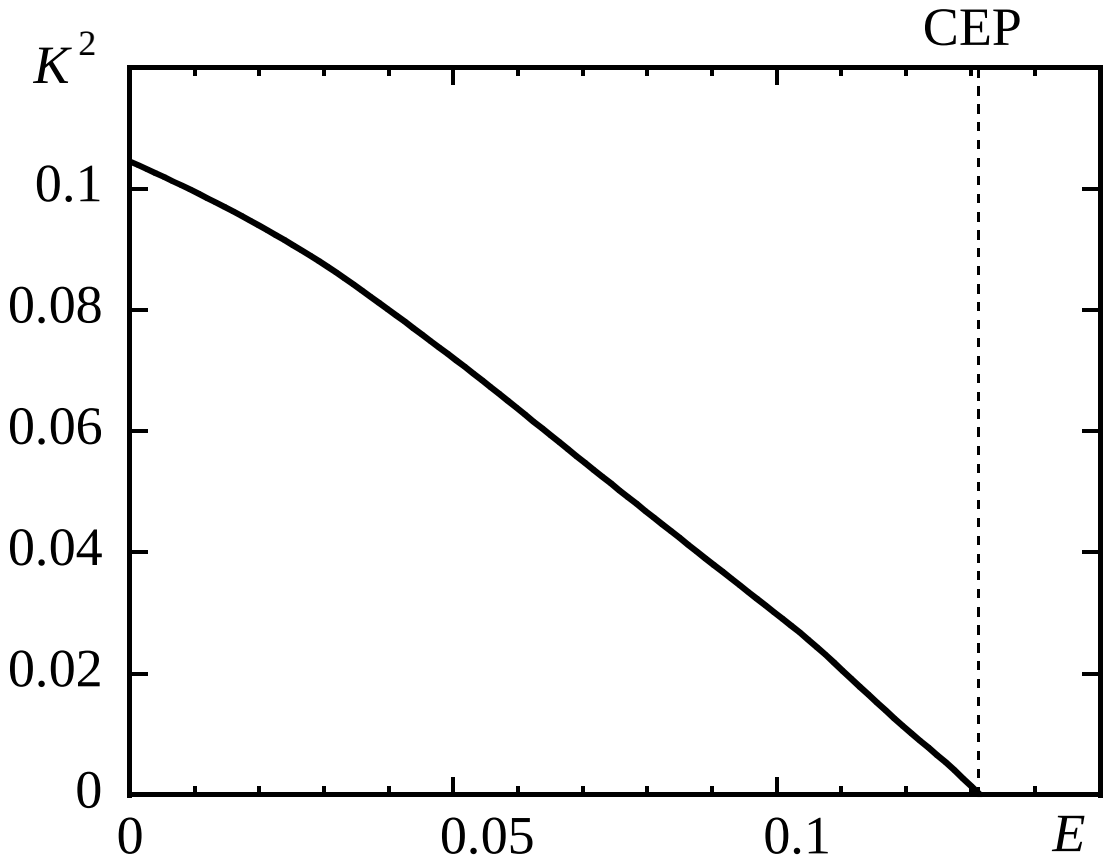

Fig. 5 M. Iwata and Y. Ishibashi